

## A library of ATTR amyloidosis patient-specific induced pluripotent stem cells for disease modelling and *in vitro* testing of novel therapeutics

Richard M. Giadone, Jessica D. Rosarda, Prithvi Reddy Akepati, Arianne C. Thomas, Batbold Boldbaatar, Marianne F. James, Andrew A. Wilson, Vaishali Sanchorawala, Lawreen H. Connors, John L. Berk, R. Luke Wiseman & George J. Murphy

To cite this article: Richard M. Giadone, Jessica D. Rosarda, Prithvi Reddy Akepati, Arianne C. Thomas, Batbold Boldbaatar, Marianne F. James, Andrew A. Wilson, Vaishali Sanchorawala, Lawreen H. Connors, John L. Berk, R. Luke Wiseman & George J. Murphy (2018) A library of ATTR amyloidosis patient-specific induced pluripotent stem cells for disease modelling and *in vitro* testing of novel therapeutics, *Amyloid*, 25:3, 148-155, DOI: [10.1080/13506129.2018.1489228](https://doi.org/10.1080/13506129.2018.1489228)

To link to this article: <https://doi.org/10.1080/13506129.2018.1489228>



© 2018 The Author(s). Published by Informa UK Limited, trading as Taylor & Francis Group.



[View supplementary material](#)



Published online: 21 Jul 2018.



[Submit your article to this journal](#)



Article views: 1334



[View related articles](#)



[View Crossmark data](#)





Citing articles: 5 [View citing articles](#)

ORIGINAL ARTICLE



## A library of ATTR amyloidosis patient-specific induced pluripotent stem cells for disease modelling and *in vitro* testing of novel therapeutics

Richard M. Giadone<sup>a</sup>, Jessica D. Rosarda<sup>b</sup>, Prithvi Reddy Akepati<sup>a</sup>, Arianne C. Thomas<sup>a</sup>, Batbold Boldbaatar<sup>c</sup>, Marianne F. James<sup>a</sup>, Andrew A. Wilson<sup>a</sup>, Vaishali Sanchorawala<sup>d,e</sup> , Lawreen H. Connors<sup>c</sup>, John L. Berk<sup>d</sup> , R. Luke Wiseman<sup>b</sup> and George J. Murphy<sup>a,e</sup>

<sup>a</sup>Center for Regenerative Medicine, Boston University School of Medicine, Boston, MA, USA; <sup>b</sup>Department of Molecular Medicine, The Scripps Research Institute, La Jolla, CA, USA; <sup>c</sup>Alan and Sandra Gerry Amyloid Research Laboratory, Amyloidosis Center, Boston University School of Medicine, Boston, MA, USA; <sup>d</sup>Amyloidosis Center, Boston University School of Medicine, Boston, MA, USA; <sup>e</sup>Section of Hematology and Oncology, Department of Medicine, Boston University School of Medicine, Boston, MA, USA

### ABSTRACT

Hereditary transthyretin amyloidosis (ATTR amyloidosis) is an autosomal dominant protein-folding disorder caused by over 100 distinct mutations in the transthyretin (*TTR*) gene. In ATTR amyloidosis, protein secreted from the liver aggregates and forms amyloid fibrils in downstream target organs, chiefly the heart and peripheral nervous system. Few animal models of ATTR amyloidosis exist and none recapitulate the multisystem complexity and clinical variability associated with disease pathogenesis in patients. Induced pluripotent stem cells (iPSCs) stand to revolutionize the way we study human development, model disease, and perhaps treat patients afflicted with highly variable multisystem diseases such as ATTR amyloidosis. Here, we fully characterize six representative iPSC lines from a library of previously reprogrammed iPSC lines and reprogrammable blood samples derived from ATTR amyloidosis patients. This unique resource, described herein, can be harnessed to study diverse disorder.

**Abbreviations:** AAT: alpha-1 antitrypsin; AFP: alpha-fetoprotein; ALB: albumin; ATTR: TTR amyloid protein; CXCR4: C-X-C chemokine receptor 4; HLC: hepatocyte-like cell; HNF4A: hepatocyte nuclear factor 4 alpha; iPSC: induced pluripotent stem cell; L55P: leucine-to-proline at position 55; L58H: leucine-to-histidine at position 58; MS: mass spectrometry; siRNA: small interfering RNA; TTR: transthyretin; V30M: valine-to-methionine at position 30; V122I: valine-to-isoleucine at position 122; WT: wild-type

### ARTICLE HISTORY

Received 23 March 2018  
Revised 8 June 2018  
Accepted 12 June 2018

### KEYWORDS

ATTR; hereditary ATTR amyloidosis; pluripotent stem cells; disease modelling; drug discovery



### Introduction


Hereditary transthyretin amyloidosis (ATTR amyloidosis) is an autosomal dominant protein folding disorder that results from over 100 described mutations in the transthyretin (*TTR*) gene. In the disease, TTR tetramers secreted by the liver, dissociate to monomers, misfold and oligomerize into proteotoxic fibrils that deposit as amyloid in downstream target tissues (e.g. the peripheral nervous system and/or cardiac tissue), inducing cell death [1]. Current therapies for ATTR amyloidosis include orthotopic liver transplantation, small molecule TTR tetramer stabilizers (e.g. diflunisal or tafamidis), and experimental small interfering RNA species (siRNAs). Conventional therapeutics rarely succeed in preventing ATTR amyloidosis disease progression due to continued formation of wild-type TTR fibrils after liver transplantation or variable and unpredictable tetramer response to different treatments [2–5]. Alternative strategies are needed to combat systemic amyloid diseases such as ATTR amyloidosis.

Patients with ATTR amyloidosis present with a wide degree of phenotypic manifestations. Some mutations preferentially

affect one organ system. For example, patients with the V122I mutation primarily exhibit cardiomyopathy, while those with the leucine-to-proline at position 55 (L55P) or valine-to-methionine at position 30 (V30M) variant present with polyneuropathy [6,7]. Interestingly, the same mutation can present with different pathologies in different individuals. The average age of onset for V30M, the most prevalent disease-causing mutation, varies greatly across different geographic locations – 33 years of age in Portugal and Japan compared with 56 years in Sweden [8]. Similarly, in Portugal, the penetrance of the V30M mutation is as high as 80% by the age of 50, but only 5–10% in Swedish carriers [9]. The highly variable genetics of the disease, especially in the context of patients with the same mutation, suggests severely underappreciated genetic modifiers that could alter disease progression. To properly understand ATTR amyloidosis pathogenesis and develop novel therapeutics, disease models must take into account the genetic and epigenetic backgrounds of patients.

Due to the multi-organ and age-related nature of disease, ATTR amyloidosis proves difficult to study in a feasible and biologically relevant way. To date, no mouse model

**CONTACT** George J. Murphy  [gjmurphy@bu.edu](mailto:gjmurphy@bu.edu)  Center for Regenerative Medicine, Boston University School of Medicine, 670 Albany Street, 2nd Floor, Boston, MA 02118, USA

 Supplemental data for this article can be accessed [here](#).

© 2018 The Author(s). Published by Informa UK Limited, trading as Taylor & Francis Group.

This is an Open Access article distributed under the terms of the Creative Commons Attribution-NonCommercial-NoDerivatives License (<http://creativecommons.org/licenses/by-nc-nd/4.0/>), which permits non-commercial re-use, distribution, and reproduction in any medium, provided the original work is properly cited, and is not altered, transformed, or built upon in any way.

accurately recapitulates human ATTR amyloidosis pathology, while bacteria-derived recombinant TTR lacks seminal post-translational modifications implicated in TTR function and disease pathogenesis [10–12].

The advent of induced pluripotent stem cells (iPSCs) capable of differentiating into any cell type in the body stand to revolutionize the way complex, systemic disorders such as ATTR amyloidosis are studied. In order to understand the pathogenesis of ATTR amyloidosis in the genetic background of the patient, we have developed an iPSC-based disease model [13]. In this model, patient-specific iPSCs are directed to differentiate into “effector” cells (hepatocyte-like cells, HLCs) by the serial addition of a number of chemically defined cytokine cocktails. Importantly, HLCs secrete wild-type and destabilized TTR variants, detectable by mass spectrometry (MS). In parallel, patient-matched iPSCs can be differentiated into “target organ” cell types – cardiomyocytes and neuronal cells. Conditioned media generated from HLCs can be used to dose target cells and downstream toxicity can be evaluated, thereby recapitulating key causative aspects of ATTR amyloidosis disease aetiology including cardiotoxicity and neurotoxicity.

Here, we describe the characterization of six representative iPSC lines from a library of iPSCs and reprogrammable blood samples from a number of ATTR amyloidosis patients. These iPSC lines are genetically identical to the individual from whom they are derived, allowing for disease modelling and the development of novel therapeutics in the exact genetic context of the patient. This unique resource can be used in combination with our laboratory’s previously described patient-specific, cell-based model [13] to facilitate studies into the genetic and epigenetic factors of the disease, and in the future, allow for pharmacogenomic assessments of novel therapeutics.

## Materials and methods

### Patient samples

To capture the phenotypic diversity of this complex disease, samples were procured from the Amyloidosis Center of Boston University School of Medicine from patients who visit the clinic from around the world. Reprogramming of material was performed on fresh samples immediately following collection or using frozen mononuclear cells that were previously collected and isolated from subjects.

### Patient consent and global distribution of created lines

All of the iPSC lines in this bank were created from patients using a progressive, state-of-the-art consent form. Informed consent for generation of iPSC lines derived from peripheral blood was obtained from all donor patients according to the Declaration of Helsinki. This consent form includes a comprehensive template that allows for the unrestricted sharing of created lines, including potential commercialization and sharing of lines with commercial entities. As a resource to investigators, this consent form has been included as a

supplementary file (Supplementary Form 1). The described library is available through the Boston University and Boston Medical Center’s Center for Regenerative Medicine ((CRoM), <http://www.bu.edu/dbin/stemcells/>) via our “Open Source Biology” initiative.

### iPSC generation and maintenance

Derivation of our iPSC library was performed as described [14–16]. Briefly, 4 ml of peripheral blood were collected from all participating individuals and the mononuclear cells (either fresh or frozen) were expanded *in vitro* and reprogrammed using the STEMCCA vector. At least, three independent clones were established, expanded and banked from each individual. For all studies described here, cells were maintained either on inactivated mouse embryo fibroblast (MEF) feeders with knockout serum replacement (KSR) supplemented media or under feeder-free conditions using mTeSR<sup>TM</sup>1 media. These studies were approved by the Institutional Review Board of Boston University.

### Immunostaining for pluripotency markers

iPSCs were grown for 5 d prior to staining. Cells were fixed with 4% paraformaldehyde (PFA) in PBS for 20 min, permeabilized with 0.1% Triton X-100 (Sigma, St. Louis, MO, Cat. no. T8787) in PBS for 10 min at room temperature, and subsequently blocked with 4% normal goat serum (Vector, San Diego, CA, Cat. no. S-1000) in PBS for 30 min. Primary antibodies (SSEA-1, SSEA-4, TRA-1-60, and TRA-1-81, EMD Millipore, Billerica, MA, Cat. no. SCR001) were diluted 1:25–1:50 in blocking solution and added to samples for 1 h. Secondary antibodies (Life Technologies, Carlsbad, CA, Cat# A21042; A11003) were diluted in PBS (1:100–1:250), and added to cells that were then incubated at room temperature for 30–60 min. Cells were stained with DAPI (Invitrogen, Carlsbad, CA, Cat. no. D1306) diluted in PBS (1:2000) and incubated for 5 min at room temperature.

### Directed differentiation of iPSCs to definitive endoderm and hepatocyte-like cells

iPSCs were passaged with Gentle Cell Dissociation (GCD) Reagent (STEMCELL Technologies, Vancouver, Canada, Cat. no. 07174) to form a single-cell suspension and counted.  $2 \times 10^6$  cells were plated in one matrigel-coated well of a standard 6-well plate in mTeSR1 supplemented with Y-27632 (10  $\mu$ M). Twenty-four hours later, media from the STEMdiff Definitive Endoderm Kit (STEMCELL Technologies, Vancouver, Canada, Cat. no. 05110) was added, and cells were cultured as per instructions for 4 d. On day 5, cells were passaged with GCD to obtain a single-cell suspension, and split 1:2 into matrigel-coated wells of a standard 6-well plate. On days 5 and 6, cells were cultured in media containing: activin A (0.05  $\mu$ g/mL), ascorbic acid (50  $\mu$ g/mL) BMP4 (0.01  $\mu$ g/mL), FGF2 (0.01  $\mu$ g/mL), VEGF (0.01  $\mu$ g/mL), L-glutamine, and monothioglycerol ( $4.5 \times 10^{-4}$  M) (Note: Day 5 media was supplemented with

10  $\mu$ M Y-27632.). Hepatic specification continued for approximately 20 d in SFD-based media as previously described with medias specific for days 7–12, 13–18, and 19–26 [17]. Days 7–12 media contained: ascorbic acid (50  $\mu$ g/mL), BMP4 (0.05  $\mu$ g/mL), FGF2 (0.01  $\mu$ g/mL), VEGF (0.01  $\mu$ g/mL), EGF (0.01  $\mu$ g/mL), TGF $\alpha$  (0.02  $\mu$ g/mL), HGF (0.1  $\mu$ g/mL), dexamethasone (0.1  $\mu$ M), L-glutamine, and monothioglycerol ( $4.5 \times 10^{-4}$  M). Day 13–18 media contained: ascorbic acid (50  $\mu$ g/mL), FGF2 (0.01  $\mu$ g/mL), VEGF (0.01  $\mu$ g/mL), EGF (0.01  $\mu$ g/mL), HGF (0.1  $\mu$ g/mL), oncostatin M (0.02  $\mu$ g/mL), Vitamin K (6  $\mu$ g/mL), gamma secretase inhibitor (1.5  $\mu$ M), DMSO (1%), dexamethasone (0.1  $\mu$ M), L-glutamine, and monothioglycerol ( $4.5 \times 10^{-4}$  M). Day 19–26 media contained: ascorbic acid (50  $\mu$ g/mL), HGF (0.1  $\mu$ g/mL), oncostatin M (0.02  $\mu$ g/mL), vitamin K (6  $\mu$ g/mL), dexamethasone (0.1  $\mu$ M), L-glutamine, and monothioglycerol ( $4.5 \times 10^{-4}$  M). For the entirety of the differentiation, cells were incubated at 37 °C, 5% O<sub>2</sub>, 5% CO<sub>2</sub>, and 90% N<sub>2</sub>.

### **Characterization of definitive endoderm and hepatic markers**

Flow cytometry was performed on days 5 and 26 of hepatic differentiation. On day 5, cells were stained with antibodies specific for cell surface markers c-Kit (ThermoFisher, Waltham, MA, Cat. no. 17–1178-42) and C-X-C chemokine receptor 4 (CXCR4) (ThermoFisher, Waltham, MA, Cat. no. 12–9999-41). Five microlitre of each antibody were added to  $5 \times 10^5$  cells. Staining was performed on ice for 30 min. For intracellular staining, on day 26, cells were fixed with 1.6% PFA (Ted Pella, Inc., Redding, CA, Cat. no. 18505) at 37 °C for 20 min. Primary antibodies for FOXA1 (Santa Cruz Technology, Santa Cruz, CA, Cat. no. 101058) and AAT (Santa Cruz Technology, Santa Cruz, CA, Cat. no. 59438) diluted 1:100 in Saponin buffer (2% FBS, 1 $\times$  Permeabilization Wash Buffer (Biolegend, San Diego, CA, Cat. no. 421002)) were added to cells and incubated for 30 min at room temperature. Secondary antibodies for FOXA1 (Jackson, West Grove, PA, Cat. no. 115–485-206) and AAT (Jackson West Grove, PA, Cat. no. 115–605-205), diluted 1:500 in Saponin buffer, were added to cells that were then incubated for 30 min at room temperature. Samples were resuspended in 0.5% bovine serum albumin (BSA) in PBS prior to analysis.

### **RNA isolation, cDNA synthesis, and qRT-PCR**

Total RNA was extracted from cells via RNeasy Mini Kit (Qiagen, Germantown, MD, Cat. no. 74104). RNA was eluted in 30  $\mu$ L RNase-free H<sub>2</sub>O. RNA was further purified via treatment with DNA removal kit (ThermoFisher, Waltham, MA, Cat. no. AM1906). One microgram purified RNA was used to generate cDNA via High-Capacity cDNA Reverse Transcription Kit (Applied Biosystems, Foster City, CA, Cat. no. 43–688-13). qRT-PCR was performed with TaqMan Universal Master Mix II, with UNG (ThermoFisher, Waltham, MA, Cat. no. 4440038). TaqMan Gene Expression Assays used include the following:  $\beta$ -actin (Hs99999903\_m1),

AAT (Hs00165475\_m1), ALB (Hs00609411\_m1), TTR (Hs00174914\_m1), hepatocyte nuclear factor 4 alpha (HNF4A) (Hs00230853\_m1), OCT4 (Hs00999634\_gH), and alpha-fetoprotein (AFP) (Hs01040598\_m1). Quantities of genes of interest were compared relative to  $\beta$ -actin levels. Fold-change was calculated via  $\Delta\Delta C_T$  method. Undetermined  $C_T$  values were taken to be 40. Samples were run in triplicate.

### **Mass spectrometric analysis of secreted TTR**

TTR was immunoprecipitated from conditioned media prepared on iPSC-derived hepatic lineages using Protein A Sepharose 4B beads (Life Technologies, Carlsbad, CA, Cat. no. 101041) cross-linked to TTR antibody (DAKO, Carlsbad, CA, Cat. no. A0002) using dimethyl pimeimide (DMP; ThermoFisher, Waltham, MA, Cat. no. 21666) according to the manufacturer protocol. Conditioned media was incubated with cross-linked TTR-Sepharose 4B beads overnight at 4 °C. Beads were then washed four times in 0.05% Saponin, 10 mM Tris, 140 mM NaCl, pH 8.0 and twice in 10 mM Tris, 140 mM NaCl, pH 8.0 prior to elution. TTR was eluted from the beads by incubating resin at 95 °C for 10 min in an SDS-lysis buffer solution (2% SDS, 1% Triton X-100, HEPES 20 mM, EDTA 1 mM, NaCl 100 mM). Eluent was removed from beads, and 100 mM dithiothreitol (DTT) was added. The eluent was then incubated again at 95 °C for 5 min. Methanol precipitation was used to remove the detergent from eluent for subsequent LC/MS analysis. A mixture of methanol:chloroform:water (4:1:3) was added in proportion to the eluent volume. Samples were centrifuged at  $21,800 \times g$  for one minute and the aqueous layer was removed. Two additional methanol washes were performed to remove residual detergent. The sample was then centrifuged at  $21,800 \times g$  for 10 min to pellet the precipitated protein. The protein pellet was dried and resuspended in 150 mM ammonium hydroxide pH 10.5. LC/MS analysis was performed on an Agilent single quadrupole mass spectrometer (Agilent Technologies, Palo Alto, CA), as previously described [18].

## **Results**

### **Establishment of an ATTR amyloidosis disease-specific iPSC library representing multiple TTR mutations and target tissue pathology**

Peripheral blood samples were procured from patients seen at the Amyloidosis Center at Boston University and Boston Medical Center in an effort to obtain a wide representation of mutations and associated disease phenotypes. This starting material was used to generate more than 30 independent iPSC lines from individuals of African-American, Caucasian, and Asian descent (Table 1). Three independent clones were generated from each patient, with starting samples representative of both genders and a wide range of ages (16–65 years old). All lines were created using previously described methodologies and met stringent quality control parameters for pluripotency and functionality [14–16] (Figure 1). Most lines in the library have been adapted to grow under feeder-



**Table 1.** Clinical data associated with ATTR amyloidosis patient-derived iPSCs.

Mutation	Sex	Ethnicity	Age of onset	Age at Dx	Symptoms	Abd. fat – Congo red results	Serum TTR levels (μg/mL)	Iron levels (μg/dL)	Treatment
I107M	F	White	NA	NA	No active disease	Neg	ND	115	NA
					No active disease	Neg		46	
					No active disease	Neg		70	
					No active disease	Neg	180	70	
V122I	M	Black	65	68	Cardiac	Neg	ND	49	Diffunisal started
L58H	M	White	53	55	Peripheral neuropathy	2+	ND	86	ND
L55P	F	White	16	–	–	–	–	–	–
V30M-1	M	Asian	39	40	Peripheral and autonomic neuropathy	2+	ND	100	Diffunisal started
						2+	270	83	Con'd
						2+	ND	71	Con'd
						2+	300	100	Con'd
V30M-2	M	White	Long-standing	49	Peripheral neuropathy	neg	ND	105	Diffunisal started

Clinical data for six representative iPSC lines from a bank of over 30 independent patient samples. Lines characterized herein represent patients of different genetic backgrounds and ethnicities. Patients from which lines were established exhibit various symptomatology (e.g., target organ affected) and severity (age of onset).

M: male; F: female; Dx: diagnosis; Abd. fat – Congo red results: presence or absence of Congo red positive fibrils in abdominal fat biopsies; NA: not applicable; ND: not determined, –: unknown.

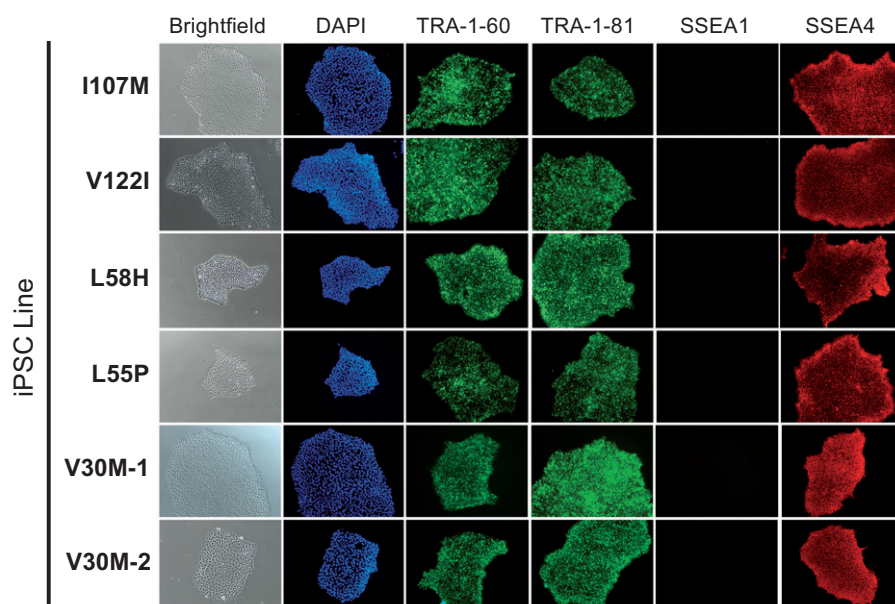


**Figure 1.** Patient-specific iPSCs express hallmark pluripotency markers. Five days after passaging, iPSC colonies from all representative lines express hallmark pluripotency cell surface markers TRA-1-60, TRA-1-81 and SSEA4. Colonies do not express murine pluripotent stem cell surface marker SSEA1. Nuclei stain positive with DAPI. Images taken at 10× magnification.

free conditions. Here, we describe the characterization of six representative patient-specific iPSC lines from the above-mentioned library.

### Characterization of capacity for directed differentiation into the hepatic lineage

Differentiation capacity characterization of banked lines was performed as we previously described using a step-wise, 2D, feeder-free, and chemically defined hepatic specification protocol [19] (Figure 2). Upon initial specification to definitive endoderm, the majority of iPSC-derived cells exhibited robust co-expression of the key markers of this developmental stage, CXCR4 and c-Kit (Figure 3). Upon further differentiation into HLCs, qRT-PCR analyses demonstrated marked upregulation of hepatic marker genes albumin

(ALB), TTR, AFP, HNF4A, and AAT accompanied by down-regulation of the pluripotency marker OCT4 (Figure 4(A)). Day 26 HLCs also exhibited protein-level co-expression of intracellular hepatic markers AFP and FOXA1, by flow cytometry (Figure 4(B)). Additionally, iPSC-derived HLCs exhibited limited protein expression of the late-stage hepatic marker, ALB (Supplemental Figure 1). The ability of iPSC-derived HLCs to achieve robust expression of adult-type markers such as ALB has not yet been achieved in directed differentiation protocols [20]. Disparities were noted between transcript and protein level expression of ALB (Figure 4(A) and Supplemental Figure 1) across HLCs derived from multiple iPSC lines. Interestingly, several post-transcriptional regulatory mechanisms have been implicated in controlling the expression of ALB in hepatocyte cell lines and animal models [21,22], potentially explaining the results presented herein.

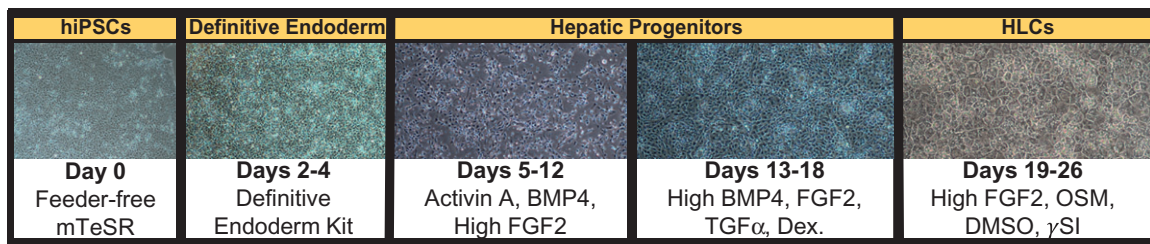


**Figure 2.** Feeder-free, chemically defined differentiation protocol for generating hepatocyte-like cells (HLCs) from patient-specific iPSCs. Schematic depicts representative photomicrographs at multiple stages of hepatic differentiation. Major cytokines included at each stage of the differentiation process are noted.

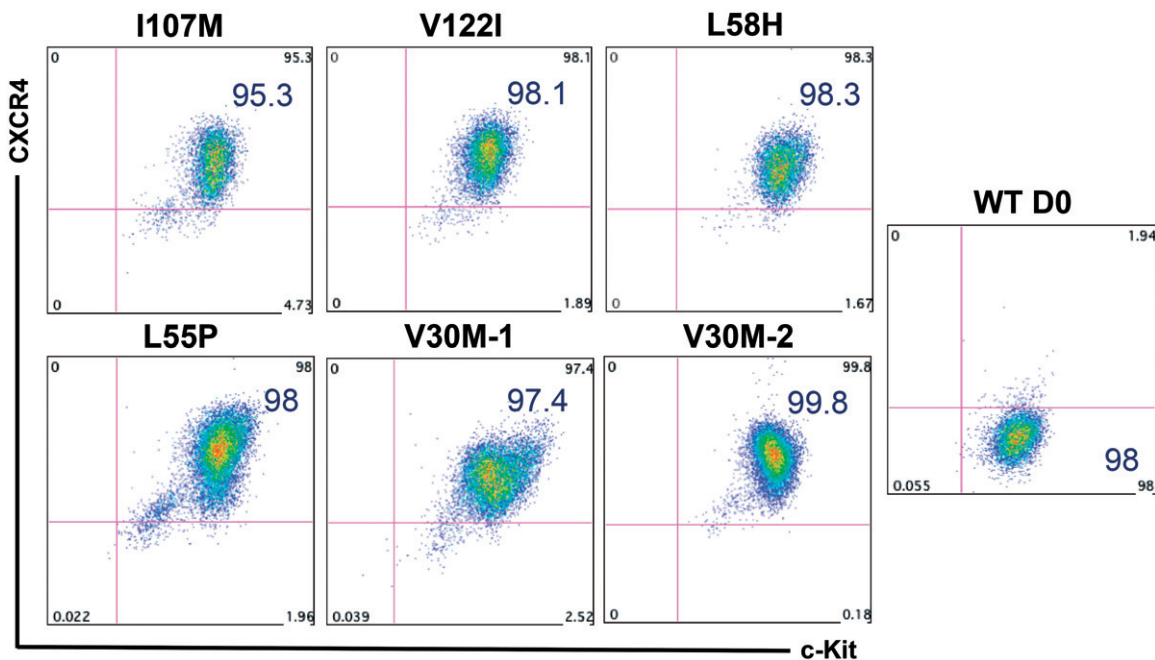


**Figure 3.** Robust generation of definitive endoderm cells from patient-specific iPSCs. After 5 d of directing iPSCs toward definitive endoderm, the majority of cells exhibit robust co-expression of the key markers of this developmental stage, CXCR4 and c-Kit. Undifferentiated cells (right) express c-Kit, but not CXCR4.

### **iPSC-derived HLCs secrete wild-type and variant-specific destabilized TTR species**

In order to assess the potential of iPSC-derived HLCs to secrete both normal and amyloidogenic TTR, we employed LC/MS characterization of conditioned media prepared on HLCs (Figure 5(A–E)). These analyses demonstrated recovery of both wild-type (WT) TTR and ATTR amyloidosis disease-specific mutant forms of TTR. Interestingly, in most cases, the relative recovery of WT species was greater than that of the disease-specific variant (Figure 5(F)).

## **Discussion**

We have generated a library of iPSCs from patients with hereditary transthyretin amyloidosis, representing multiple TTR mutations and target tissue pathology for applications related to disease modelling and drug discovery. These fully characterized lines, along with accompanying functional data are now freely available, providing a resource to aid in the understanding of the complex aetiology of the disorder.

Drug development is an extremely expensive and time-consuming process that requires stringent specificity, potency,

and toxicity validation of potential novel therapeutics. Traditionally, the drug discovery pathway proceeds from *in vitro* testing in cell-based assays in the lab to *in vivo* testing in animal models, followed by three phases of clinical validation. Potential therapeutics are not usually extensively tested in humans until phase I and II clinical trials, which can occur many years after initial drug discovery. If *in vitro* testing is performed on human cells prior to clinical trials, these cells are typically immortalized cell lines, which have undergone genetic alterations to ensure their immortalization, possibly compromising the fidelity of drug screens. The use of immortalized cells lines is a common cause of high attrition rates for drug development, as *in vitro* and subsequent animal model data may not predict clinical effect [23]. iPSCs provide a revolutionary platform for pre-clinical drug screening in genetically diverse patient populations, such as the broad spectrum of patients suffering from ATTR amyloidosis. It is also possible to obtain toxicity and efficacy data in multiple cell types from the same individual, all before human clinical trials [24–26]. Recently, iPSCs have been used to model diseases as well as screen drugs for the treatment of amyotrophic lateral sclerosis [27], spinal muscular atrophy [18], long QT syndrome [28], familial dysautonomia [29], and familial TTR-amyloidosis [13].

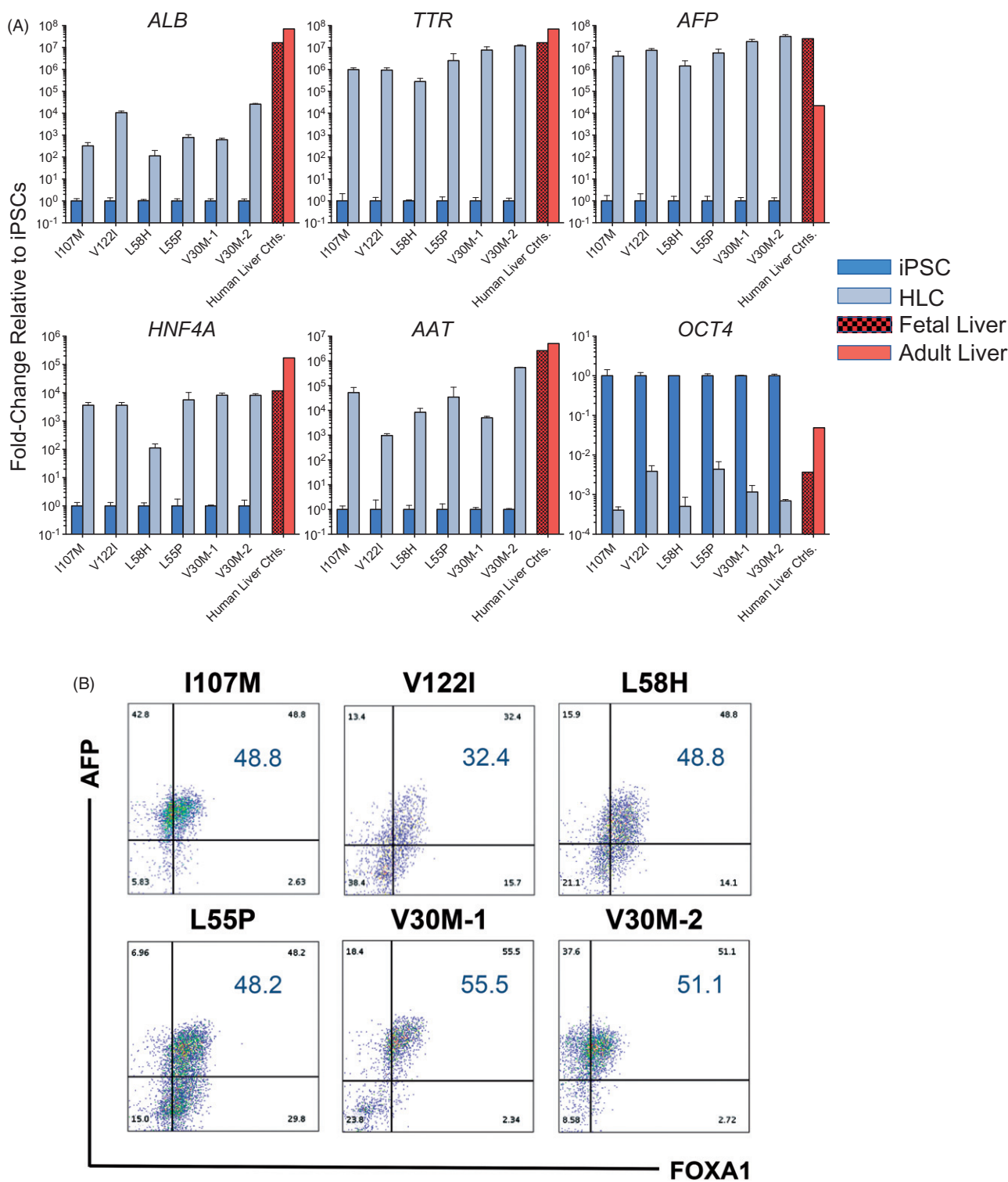


**Figure 4.** iPSC-derived HLCs upregulate hallmark hepatic markers and downregulate pluripotency markers. (A) On day 26 of hepatic differentiation to HLCs, qRT-PCR analyses demonstrate marked upregulation of hepatic marker genes *ALB*, *TTR*, *AFP*, *HNF4A* and alpha-1 antitrypsin (*AAT*) accompanied by downregulation of the pluripotency marker *OCT4*. Human fetal and adult liver controls are included for comparison. (B) Day 26, HLCs exhibit protein-level expression of intracellular hepatic markers AFP and FOXA1 by flow cytometry.

Many researchers have already taken steps to demonstrate the efficacy of stem cell-generated cells in both modelling diseases and screening for novel therapeutics [30], thus initiating iPSCs into the drug discovery phase of therapeutic development.

ATTR amyloidosis is phenotypically diverse, a quality that arises from the many causal mutations in combination

with variable genetic backgrounds in the diverse patient population that suffers from the disorder. Since there are still many unknown regulators of *TTR* expression, finding drugs that will be efficacious in patients with a variety of genetic backgrounds would be ideal, and the creation of the described iPSC bank will contribute to this effort.

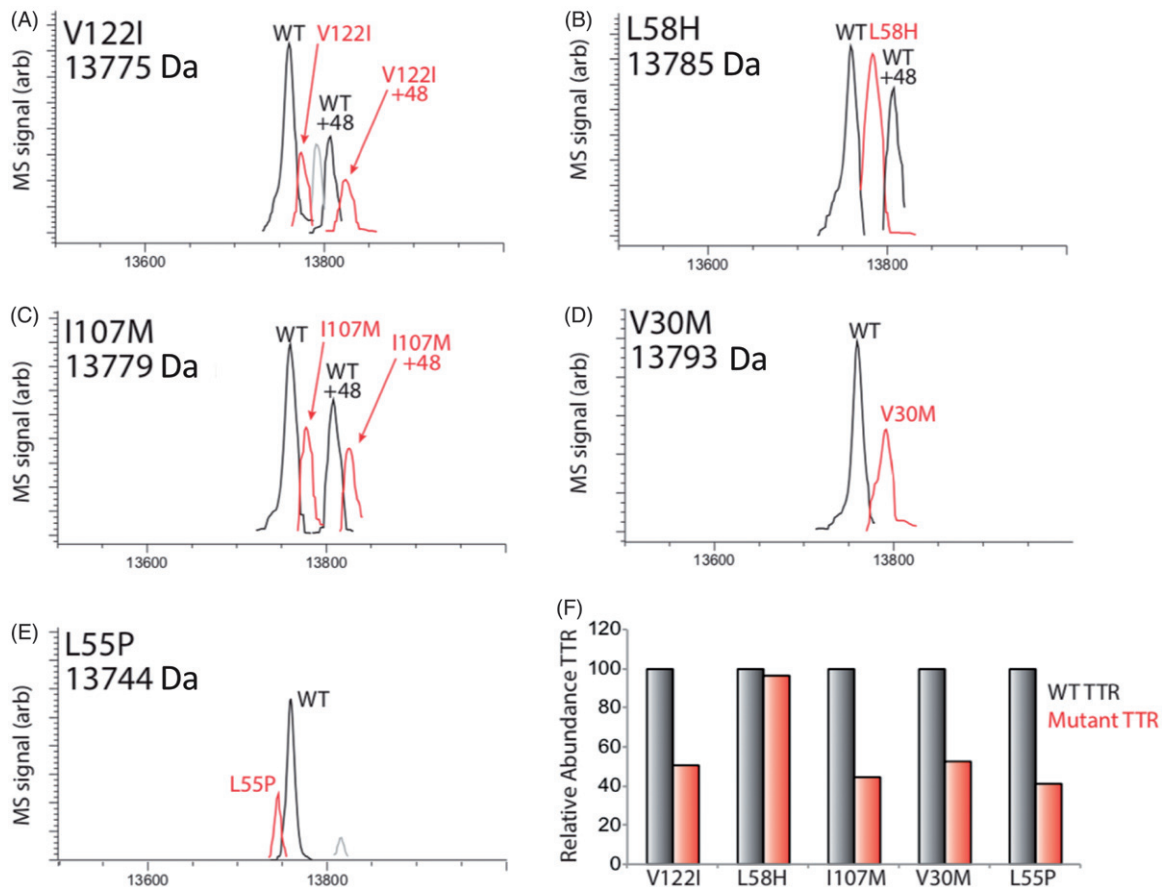


**Figure 5.** LC/MS characterization of TTR mutants secreted from HLCs. (A–E) LC/MS deconvolution spectra showing recovery of WT TTR or specific TTR mutant from TTR IPs of conditioned media prepared on iPSC-derived HLCs. A +48 peak was observed in some TTR IPs for both WT and mutant variants, reflecting oxidation of TTR. The mass of each mutant is shown, while the mass of WT TTR was determined to be  $13,761 \pm 2$  Da. Additional peaks observed in (A) and (C) likely depict a doubly oxidized TTR species and unidentified species of negligible abundance, respectively (Note: Bovine TTR (13555) was detected in these experiments, but we omitted this peak from the above spectra for clarity.). (F) Bar graph showing the relative recovery of mutant TTR compared with WT TTR (right and left bars, respectively) in the IPs shown in panels A–E. The relative recovery of oxidized mutant TTR relative to oxidized WT TTR showed similar recoveries, but are not included here.

## Disclosure statement

The authors report no conflict of interest.

## Funding

This work was funded by National Institute of Diabetes and Digestive and Kidney Diseases [grant number: 1R01DK102635-01], National Institutes of Health [grant numbers: R01AG031804, 2R56AG031804-06A1] and also by the Boston University School of Medicine Young Family Amyloid Research Fund.

## ORCID

Vaishali Sanchorawala <http://orcid.org/0000-0002-6307-2445>

John L. Berk <http://orcid.org/0000-0002-1768-2373>

## References

- [1] Blancas-Mejia LM, Ramirez-Alvarado M. Systemic amyloidoses. *Annu Rev Biochem.* 2013;82:745–774.
- [2] Berk JL, Suhr OB, Obici L, et al. Repurposing diflunisal for familial amyloid polyneuropathy: a randomized clinical trial. *JAMA.* 2013;310:2658–2667.
- [3] Ando Y, Sekijima Y, Obayashi K, et al. Effects of tafamidis treatment on transthyretin (TTR) stabilization, efficacy, and safety in Japanese patients with familial amyloid polyneuropathy (TTR-FAP) with Val30Met and non-Val30Met: a phase III, open-label study. *J Neurol Sci.* 2016;362:266–271.
- [4] Maurer MS, Elliott P, Merlini G, et al. Design and rationale of the phase 3 ATTR-ACT clinical trial (Tafamidis in Transthyretin Cardiomyopathy Clinical Trial). *Circ Heart Fail.* 2017;10. DOI:10.1161/CIRCHEARTFAILURE.116.003815
- [5] Butler JS, Chan A, Costelha S, et al. Preclinical evaluation of RNAi as a treatment for transthyretin-mediated amyloidosis. *Amyloid.* 2016;23:109–118.
- [6] Lashuel HA, Wurth C, Woo L, et al. The most pathogenic transthyretin variant, L55P, forms amyloid fibrils under acidic conditions and protofilaments under physiological conditions. *Biochemistry.* 1999;38:13560–13573.
- [7] Dzung JN, Anderson LJ, Whelan CJ, et al. Cardiac transthyretin amyloidosis. *Heart.* 2012;98:1546–1554.
- [8] Hellman U, Alarcon F, Lundgren HE, et al. Heterogeneity of penetrance in familial amyloid polyneuropathy, ATTR Val30Met, in the Swedish population. *Amyloid.* 2008;15:181–186.
- [9] Parman Y, Adams D, Obici L, et al. Sixty years of transthyretin familial amyloid polyneuropathy (TTR-FAP) in Europe: where are we now? A European network approach to defining the epidemiology and management patterns for TTR-FAP. *Curr Opin Neurol.* 2016;29:3–13.
- [10] Buxbaum JN. Animal models of human amyloidosis: are transgenic mice worth the time and trouble? *FEBS Lett.* 2009;583:2663–2673.
- [11] Henze A, Homann T, Serteser M, et al. Post-translational modifications of transthyretin affect the triiodothyronine-binding potential. *J Cell Mol Med.* 2015;19:359–370.



- [12] Vilà-rico M, Colomé-calls N, Martín-castel L, et al. Quantitative analysis of post-translational modifications in human serum transthyretin associated with familial amyloidotic polyneuropathy by targeted LC-MS and intact protein MS. *J Proteomics*. 2015;127:234–246.
- [13] Leung A, Nah SK, Reid W, et al. Induced pluripotent stem cell modeling of multisystemic, hereditary transthyretin amyloidosis. *Stem Cell Rep*. 2013;1:451–463.
- [14] Sommer CA, Stadtfeld M, Murphy GJ, et al. Induced pluripotent stem cell generation using a single lentiviral stem cell cassette. *Stem Cells*. 2009;27:543–549.
- [15] Somers A, Jean JC, Sommer CA, et al. Generation of transgene-free lung disease-specific human induced pluripotent stem cells using a single excisable lentiviral stem cell cassette. *Stem Cells*. 2010;28:1728–1740.
- [16] Sommer AG, Rozelle SS, Sullivan S, et al. Generation of human induced pluripotent stem cells from peripheral blood using the STEMCCA lentiviral vector. *J Vis Exp*. 2012. DOI:10.3791/4327
- [17] Gouon-Evans V, Boussemart L, Gadue P, et al. BMP-4 is required for hepatic specification of mouse embryonic stem cell-derived definitive endoderm. *Nat Biotechnol*. 2006;24:1402–1411.
- [18] Ebert AD, Yu J, Rose FF, et al. Induced pluripotent stem cells from a spinal muscular atrophy patient. *Nature*. 2009;457:277–280.
- [19] Wilson AA, Ying L, Liesa M, et al. Emergence of a stage-dependent human liver disease signature with directed differentiation of alpha-1 antitrypsin-deficient iPS cells. *Stem Cell Rep*. 2015;4:873–885.
- [20] Baxter M, Withey S, Harrison S, et al. Phenotypic and functional analyses show stem cell-derived hepatocyte-like cells better mimic fetal rather than adult hepatocytes. *J Hepatol*. 2015;62:581–589.
- [21] Beauchamp RD, Sheng HM, Alam T, et al. Posttranscriptional regulation of albumin and a-fetoprotein messenger RNA by transforming growth factor-PI requires de novo RNA and protein synthesis. *J Mol Endocrinol*. 1992;6:1789–1796.
- [22] Kazmaier M, Brüning E, Ryffel GU. Post-transcriptional regulation of albumin gene expression in *Xenopus* liver. *EMBO J*. 1985;4:1261–1266.
- [23] Kola I, Landis J. Can the pharmaceutical industry reduce attrition rates? *Nat Rev Drug Discov*. 2004;3:711–715.
- [24] Lian Q, Chow Y, Esteban MA, et al. Future perspective of induced pluripotent stem cells for diagnosis, drug screening and treatment of human diseases. *Thromb Haemost*. 2010;104:39–44.
- [25] Chun YS, Byun K, Lee B. Induced pluripotent stem cells and personalized medicine: current progress and future perspectives. *Anat Cell Biol*. 2011;44:245–255.
- [26] Deshmukh RS, Kovacs KA, Dinnyes A. Drug discovery models and toxicity testing using embryonic and induced pluripotent stem-cell-derived cardiac and neuronal cells. *Stem Cells Int*. 2012;2012:379569.
- [27] Egawa N, Kitaoka S, Tsukita K, et al. Drug screening for ALS using patient-specific induced pluripotent stem cells. *Sci Transl Med*. 2012;4:145ra104.
- [28] Itzhaki I, Maizels L, Huber I, et al. Modelling the long QT syndrome with induced pluripotent stem cells. *Nature*. 2011;471:225–229.
- [29] Lee G, Papapetrou EP, Kim H, et al. Modelling pathogenesis and treatment of familial dysautonomia using patient-specific iPSCs. *Nature*. 2009;461:402–406.
- [30] McNeish J, Roach M, Hambor J, et al. High-throughput screening in embryonic stem cell-derived neurons identifies potentiators of alpha-amino-3-hydroxyl-5-methyl-4-isoxazole-propionate-type glutamate receptors. *J Biol Chem*. 2010;285:17209–17217.